

Surface spectral function in the superconducting state of a topological insulator

Lei Hao and T. K. Lee

Institute of Physics, Academia Sinica, NanKang, Taipei 11529, Taiwan

(Received 31 December 2010; revised manuscript received 26 February 2011; published 18 April 2011)

We discuss the surface spectral function of superconductors realized from a topological insulator, such as the copper-intercalated Bi_2Se_3 . These functions are calculated by projecting bulk states to the surface for two different models proposed previously for the topological insulator. Dependence of the surface spectra on the symmetry of the bulk pairing order parameter is discussed with particular emphasis on the odd-parity pairing. Exotic spectra such as an Andreev bound state connected to the topological surface states are presented.

DOI: [10.1103/PhysRevB.83.134516](https://doi.org/10.1103/PhysRevB.83.134516)

PACS number(s): 74.20.Rp, 73.20.At, 74.45.+c

I. INTRODUCTION

Recently, a new state of matter, the topological insulator, has attracted much theoretical and experimental attention.^{1–15} It has an electronic structure dominated by spin-orbit coupling, which is a band insulator with a well-defined gap in the bulk but can host an odd number of Dirac cones protected by time-reversal symmetry on the surface.^{1,2,7} The intrinsic spin-orbit coupling makes it promising for spintronics applications.¹⁰ The proximity-induced superconducting state on the topological insulator surface by a deposited superconductor was proposed to create Majorana fermions,¹⁶ which may provide a new way to realize the topological quantum computation.^{17,18} Lately, the realization of a superconducting state in a typical topological insulator Bi_2Se_3 by intercalating Cu between adjacent quintuple units ($\text{Cu}_x\text{Bi}_2\text{Se}_3$) makes the system even more attractive.^{19,20} The large diamagnetic response shows that the pairing is mainly of bulk character. In another topological insulator Bi_2Te_3 , the application of high pressure also turns the material into a superconducting state.^{21,22}

Since the superconductivity is bulk and intrinsic to the material, if a zero-energy surface Majorana fermion mode exists, it would be easier to manipulate as compared to that induced by proximity effect, as it would not experience the interface roughness or mismatch common to a junction-type device. Possible nontrivial odd-parity pairing in $\text{Cu}_x\text{Bi}_2\text{Se}_3$ is proposed and analyzed by Fu and Berg.²³ It was argued that only if a bulk gap opens and the bulk pairing is odd in parity, would zero-energy Andreev bound states appear in the surface spectrum. However, their analysis was concentrated on the case when the chemical potential is much larger than the gap and the topological surface states are already merged into the continuum conduction band. A similar analysis was put forward by Sato.²⁴

Despite the above works, a detailed theoretical analysis of the surface spectrum in the superconducting phase arising from a topological insulator is still lacking. In particular, not much is reported for the situation when the chemical potential is only slightly larger than the insulating gap and both topological surface states (or the surface conduction band²⁰) and the continuum bulk conduction band are present but separated. Since the surface spectrum is central to the topological properties of a material both in the normal and in the superconducting state, which is also directly accessible by experimental techniques such as ARPES²⁰ and STM,²⁵ it is highly desirable to make a detailed study of them. This will

help to understand better superconductivity in systems with nontrivial topological band structure.

We focus on two questions in this paper. One is the effect of superconducting pairing on the topological surface states²⁰ present in the normal state. The other is the existence of surface Andreev bound states. We have noticed that two different models^{12,26} are often used indiscriminately in the literature. They have the same normal state energy spectra but may be different in the superconducting state. We thus present our results for both of them. What happens to the topological surface states when pairing is introduced in the bulk depends on the orbital character of the topological surface state and on the bulk pairing symmetry. Only when the continuum part of the band opens a full gap and the topological surface states, while separated from the bulk conduction band, do not open a gap for an odd-parity pairing, would a gapless Andreev bound state appear. We find that the orbital characters of the topological surface states are different for the two models. For a certain bulk pairing symmetry, it is possible that the topological surface state of one model opens a gap while that of the other model is still intact. The existence of Andreev bound states, the most important indication of nontrivial topological order in the superconducting phase, is thus expected to be also related to the orbital character of the topological surface states. We show that the interplay between the continuum bulk conduction band and the topological surface states produces a ring or a segment of zero-energy states in addition to the Andreev bound states depending on the symmetry of bulk pairing order parameters.

II. MODELS AND THE NORMAL STATE SURFACE MODES

In the following, when we talk about topological insulators, we are mainly referring to Bi_2Se_3 , which shows a well-defined Dirac cone structure for the topological surface states.^{11,12,27} The model we consider below could be easily generalized to study other topological insulators such as TlBiSe_2 ^{28,29} and $\text{Bi}_2\text{Te}_2\text{Se}$.^{30,31}

The band structure of $\text{Cu}_x\text{Bi}_2\text{Se}_3$ is similar to that of Bi_2Se_3 , the most essential part of which consists of two p_z orbitals on the top and bottom Se layers hybridized with neighboring Bi p_z orbitals, in each quintuple Bi_2Se_3 unit.^{12,23} In the presence of spin-orbit coupling, the normal state has four degrees of freedom. Labeling the two orbitals concentrating mainly on the top and bottom (looking along the $-z$ direction) Se layers of the various Bi_2Se_3 quintuple units as the first and second orbital, the basis is taken as $\psi_{\mathbf{k}} = [c_{1\mathbf{k}\uparrow}, c_{2\mathbf{k}\uparrow}, c_{1\mathbf{k}\downarrow}, c_{2\mathbf{k}\downarrow}]^T$.

The models can be written compactly in the following matrix form:^{12,23,26}

$$H(\mathbf{k}) = \epsilon_0(\mathbf{k})I_{4 \times 4} + \sum_{i=0}^3 m_i(\mathbf{k})\Gamma_i. \quad (1)$$

$I_{4 \times 4}$ is the fourth-order unit matrix, giving rise to a topologically trivial shift of the energy bands and will be neglected in most of our following analysis. In terms of the 2×2 Pauli matrices s_i ($i = 0, \dots, 3$) in the spin subspace and σ_i ($i = 0, \dots, 3$) in the orbital subspace, the first three Dirac matrices are defined as^{12,26} $\Gamma_0 = s_0 \otimes \sigma_1$, $\Gamma_1 = s_1 \otimes \sigma_3$, $\Gamma_2 = s_2 \otimes \sigma_3$. As regards Γ_3 , there are presently two different choices: (I) $s_0 \otimes \sigma_2$ ^{23,26,32} and (II) $s_3 \otimes \sigma_3$,^{12,33–36} which define the two models that will be considered in parallel in the following discussion. Since Bi_2Se_3 is inversion symmetric, parity can be used to label states. Some papers adopt the bonding and antibonding states of the two orbitals defined above as the orbital basis.^{12,32–36} The corresponding models can be obtained in terms of a simple unitary transformation performed in the orbital subspace. Note that the two different models give the same bulk band dispersion $\epsilon_{\pm}(\mathbf{k}) = \epsilon_0(\mathbf{k}) \pm \sqrt{\sum_{i=0}^3 m_i^2(\mathbf{k})}$, with each of two eigen-energies twofold Kramers degenerate due to the time-reversal symmetry and the inversion symmetry of the model. However, we will show in the following that they are essentially two physically distinct models.

For the coefficients $\epsilon_0(\mathbf{k})$ and $m_i(\mathbf{k})$ ($i = 0, 1, 2, 3$), there are different possible parametrizations which coincide with each other close to the Γ point.^{12,14,26,37} Without loss of generality, we take the parametrizations of Wang *et al.*²⁶ Since the diagonal term $\epsilon_0(\mathbf{k})$ proportional to the unit matrix does not affect the topological characters, it is ignored here. The system is defined on a hypothetical bilayer hexagonal lattice stacked along the z axis, respecting the in-plane hexagonal symmetry of the original Bi_2Se_3 lattice. With the three independent in-plane nearest-neighbor unit vectors defined as $\hat{b}_1 = (\frac{\sqrt{3}}{2}, \frac{1}{2})$, $\hat{b}_2 = (-\frac{\sqrt{3}}{2}, \frac{1}{2})$, and $\hat{b}_3 = (0, -1)$, we have $m_0(\mathbf{k}) = m + 2t_z(1 - \cos k_z) + 2t(3 - 2\cos\frac{\sqrt{3}}{2}k_x \cos\frac{1}{2}k_y - \cos k_y)$, $m_1(\mathbf{k}) = 2\sqrt{3}t \sin\frac{\sqrt{3}}{2}k_x \cos\frac{1}{2}k_y$, $m_2(\mathbf{k}) = 2t(\cos\frac{\sqrt{3}}{2}k_x \sin\frac{1}{2}k_y + \sin k_y)$, and $m_3(\mathbf{k}) = 2t_z \sin k_z$. The in-plane and out-of-plane lattice parameters³⁸ are taken as length units in the above expression, that is, $a = c = 1$. When $mt_z < 0$ and $mt < 0$, the parametrization defined above²⁶ and the parametrization in the small \mathbf{k} effective model proposed by Zhang *et al.*¹² describe qualitatively the same physics. With this parametrization, it is easy to see that the model has the inversion symmetry $PH(\mathbf{k})P^{-1} = H(-\mathbf{k})$, where the inversion operator is defined as $P = s_0 \otimes \sigma_1$.⁸

Now, we clarify the differences between models I and II by their surface states, which is one of the most important signatures of nontrivial topological order in the system. Close to the Γ point in the BZ, we take $m_{i=0,\dots,3}(\mathbf{k}) = \{m + \frac{3}{2}t(k_x^2 + k_y^2) + t_z k_z^2, 3tk_x, 3tk_y, 2t_z k_z\}$, in which $t > 0$, $t_z > 0$, and $m < 0$. Consider a sample occupying the lower half space $z \leq 0$. The possible surface states localized close to $z = 0$ is searched by solving a set of four coupled second-order differential equations,

$$H(k_x = k_y = 0, k_z \rightarrow -i\partial_z)\Psi(z) = E\Psi(z), \quad (2)$$

together with the open boundary condition $\Psi(z)|_{z=0} = \Psi(z)|_{z=-\infty} = 0$.^{34,35} $\Psi(z)$ is the four-component eigenvector and E is the energy of the surface mode. We look for the zero-energy states and hence set $E = 0$.³⁴

For model I with $\Gamma_3 = s_0 \otimes \sigma_2$, the up and down spin degrees of freedom are decoupled from each other. The wave function can thus be written as $\Psi(z) = [u_1(z), u_2(z), u_3(z), u_4(z)]^T = [\chi_{\uparrow}(z), \chi_{\downarrow}(z)]^T$. The two spin components of the zero-energy mode satisfy the same equation as (s is \uparrow or \downarrow for the two spin degrees of freedom)

$$[(m - t_z \partial_z^2)\sigma_1 - 2it_z \partial_z \sigma_2]\chi_s(z) = 0. \quad (3)$$

The two degenerate zero-energy surface modes for $z \leq 0$ are obtained as

$$\Psi_{\alpha}(z) = C\eta_{\alpha}(e^{z/\xi_{+}} - e^{z/\xi_{-}}), \quad (4)$$

where $\alpha = 1$ or 2 , C is a normalization constant, and $\xi_{\pm}^{-1} = 1 \pm \sqrt{1 + m/t_z} \cdot 1/\text{Re}[\xi_{\pm}^{-1}]$ (“Re” means taking the real part of a number) are the two penetration depths of the surface modes into the bulk. The two unit vectors are $(\eta_1)_{\beta} = \delta_{\beta 1}$ and $(\eta_2)_{\beta} = \delta_{\beta 3}$, where $\delta_{\alpha\beta}$ is one for $\alpha = \beta$ and zero otherwise. Taking $\{\Psi_1, \Psi_2\}$ as the two bases, the effective model for the surface states is obtained by considering the k_x and k_y dependent terms in the original model as perturbations, which are

$$\Delta H_{3D} = \frac{3}{2}t(k_x^2 + k_y^2)\Gamma_0 + 3t(k_x\Gamma_1 + k_y\Gamma_2). \quad (5)$$

Supposing the two bases are normalized, the effective model for the surface states is¹²

$$H_{\text{eff}}(\mathbf{k}) = 3t(k_x s_x + k_y s_y), \quad (6)$$

where s_x and s_y are the first and second Pauli matrices. Since the two bases both have definite spin characters, s_x and s_y in the above equation can also be considered as acting in the spin subspace. The most salient feature of this model is that the corresponding surface states have contributions only from the first orbital. When we consider a sample occupying $z \geq 0$, the surface states at $z = 0$ would arise only from the second orbital.

We now study model II for $\Gamma_3 = s_3 \otimes \sigma_3$. We still consider a sample situated at $z \leq 0$ with the open boundary conditions. Following exactly the same steps as for the first model, we obtain the two degenerate zero-energy surface states as

$$\Phi_{\alpha}(z) = C\eta_{\alpha}(e^{z/\xi_{+}} - e^{z/\xi_{-}}), \quad (7)$$

where $\alpha = 1$ or 2 , C is a normalization constant, and ξ_{\pm} are defined identically as above. However, the two unit basis vectors are quite different from the first model and are $\eta_1 = \frac{1}{\sqrt{2}}[1, -i, 0, 0]^T$ and $\eta_2 = \frac{1}{\sqrt{2}}[0, 0, -i, 1]^T$. The two-dimensional effective model for the surface states is also a bit different at least formally,

$$H_{\text{eff}}(\mathbf{k}) = 3t\hat{z} \cdot (\mathbf{k} \times \mathbf{s}) = 3t(k_x s_y - k_y s_x). \quad (8)$$

The Pauli matrices s_x and s_y act in the twofold degenerate basis of the zero-energy surface states which both have definite spin characters. For a general two-dimensional wave vector, the surface state would be a linear combination of all four spin-orbital bases.

Thus there are qualitative differences between the two models which were used indiscriminately in the literature for Bi_2Se_3 .^{12,23,26,32–36} While only one orbital contributes to the surface states for model I, both orbitals contribute in equal weight to the surface states for model II. On the other hand, the effective model of the surface states has the same spin-orbital coupled form as the linear k_x and k_y terms in the original three-dimensional model for model I. However, the effective model is changed from $\mathbf{k} \cdot \mathbf{s}$ to $\hat{z} \cdot (\mathbf{k} \times \mathbf{s})$ for model II. We have verified that, if we change the in-plane spin-orbit coupling of models I and II from $\mathbf{k} \cdot \mathbf{s}$ to $\hat{z} \cdot (\mathbf{k} \times \mathbf{s})$, the resulting effective model of the surface states will have the form $\hat{z} \cdot (\mathbf{k} \times \mathbf{s})$ for model I but will be switched to $\mathbf{k} \cdot \mathbf{s}$ for model II.

Before ending this section, we would like to point out that both the k_z -linear term in $m_3(\mathbf{k})$ and the k_z -square term in $m_0(\mathbf{k})$ are essential to obtain the zero-energy surface modes. If we omit the k_z^2 term in $m_0(\mathbf{k})$, it is easy to verify that the gapless surface states no longer exist. This is related to the fact that band inversion is essential to the appearance of nontrivial topological surface states,^{2,39} which can only occur in the presence of the k_z^2 term for $k_x = k_y = 0$.

III. SUPERCONDUCTING STATE SPECTRAL FUNCTION

A. Surface Green's functions in the superconducting state

The realization of the superconducting state in $\text{Cu}_x\text{Bi}_2\text{Se}_3$ ^{19,20} has brought about excitement that a nontrivial topological superconducting state might be realized in this system, in which topologically protected gapless surface states traverse the bulk superconducting gap.^{23,24,40} The recent realization of a superconducting phase in Bi_2Te_3 under high pressure^{21,22} makes the Bi_2X_3 (X is Se or Te) material a very promising candidate system to realize topologically nontrivial superconducting phases.^{23,24,40}

The normal state of the topological insulator is marked by the presence of topological surface states inside the bulk gap. These gapless topological surface states are well separated from the bulk conduction band at low energies and become indistinguishable for energies much higher than the conduction band minimum. Depending on the doped charge density the superconducting state could occur with the chemical potential either deep in the bulk conduction band or in the intermediate region where the topological surface states are well separated from the bulk conduction band.²⁰ In the latter case, the coupling between the continuum bulk states and the isolated topological surface states may cause some new interesting phenomena. Thus this intermediate region is what we will concentrate on below. Furthermore, the actual pairing symmetries of the superconducting $\text{Cu}_x\text{Bi}_2\text{Se}_3$ and Bi_2Te_3 are presently unknown.^{19–22} Thus we will examine cases with different pairing symmetries in the hope of providing clues to identify the pairing symmetry and the role contributed by the topological surface states.

In the following, we will study the surface spectral function to see possible nontrivial topological properties arising from the normal phase topological order which is subject to a certain bulk pairing. The surface spectral function, which could be obtained from the surface Green's function, has been studied by ARPES²⁰ and STM²⁵ to give important information on the

topological properties of the system. In the superconducting state, we expect to see some surface Andreev bound states if a certain superconducting order is realized in the material.

In the presence of a surface perpendicular to the z axis, k_x and k_y are good quantum numbers, and k_z is replaced by $-i\partial_z$ as we shall search for surface states. We then discretize the z coordinate and turn the whole sample ($z \leq 0$) with a surface at $z = 0$ to a coupled quintuple-layer system. Labeling each separate quintuple unit with an integer index n , and making the substitutions $\partial_z \psi_n(z) = \frac{1}{2}[\psi_{n+1} - \psi_{n-1}]$ and $\partial_z^2 \psi_n(z) = \psi_{n+1} + \psi_{n-1} - 2\psi_n$ (c is set as length unit along z axis), the Hamiltonian now consists of the intralayer terms and the interlayer hopping terms, $\hat{H} = \hat{H}_{\parallel} + \hat{H}_{\perp}$. The intralayer part of the model is $\hat{H}_{\parallel} = \sum_{n\mathbf{k}} \psi_{n\mathbf{k}}^\dagger h_{xy}(\mathbf{k}) \psi_{n\mathbf{k}}$, in which

$$h_{xy}(\mathbf{k}) = m'_0(\mathbf{k})\Gamma_0 + m_1(\mathbf{k})\Gamma_1 + m_2(\mathbf{k})\Gamma_2. \quad (9)$$

$m_1(\mathbf{k})$ and $m_2(\mathbf{k})$ are the same as those in the bulk model. $m'_0(\mathbf{k})$ is obtained from $m_0(\mathbf{k})$ by first expanding it up to the square term of k_z and then replacing the term proportional to k_z^2 from Ck_z^2 to $2C$.

The interlayer hopping term is $\hat{H}_{\perp} = \sum_{n\mathbf{k}} \psi_{n\mathbf{k}}^\dagger h_z \psi_{n+1,\mathbf{k}} + \text{H.c.}$ In terms of the parametrizations of Wang *et al.*,²⁶ we have

$$h_z = -t_z(\Gamma_0 + i\Gamma_3). \quad (10)$$

Since the Γ_3 matrix now appears only in the h_z part of the coupled-layers system, the difference between the two models enters only through the interlayer hopping term.

Now introduce superconducting pairing and define the Nambu basis as $\phi_{n\mathbf{k}}^\dagger = [\psi_{n\mathbf{k}}^\dagger, \psi_{n-\mathbf{k}}^T]$. The intra-layer part of the Bogoliubov de Gennes (BdG) Hamiltonian is then $\hat{H}_{\parallel}^{\text{SC}} = \sum_{n\mathbf{k}} \phi_{n\mathbf{k}}^\dagger H_{\text{SC}}(\mathbf{k}) \phi_{n\mathbf{k}}$, in which⁴¹

$$H_{\text{SC}}(\mathbf{k}) = \begin{pmatrix} h_0(\mathbf{k}) & \underline{\Delta}(\mathbf{k}) \\ -\underline{\Delta}^*(-\mathbf{k}) & -h_0^*(-\mathbf{k}) \end{pmatrix}, \quad (11)$$

where $h_0(\mathbf{k}) = h_{xy}(\mathbf{k}) - \mu I_{4 \times 4}$, with μ the chemical potential. $\underline{\Delta}(\mathbf{k})$ is the 4×4 pairing matrix. Ignoring the possibility of interlayer pairing, the interlayer hopping terms are $\hat{H}_{\perp}^{\text{SC}} = \sum_{n\mathbf{k}} \phi_{n\mathbf{k}}^\dagger H_z \phi_{n+1,\mathbf{k}} + \text{H.c.}$, in which

$$H_z = \begin{pmatrix} h_z & 0 \\ 0 & -h_z^* \end{pmatrix}. \quad (12)$$

Once the pairing order is given, the surface spectral function is obtained from the retarded surface Green's functions, which could be calculated in terms of the standard transfer matrix method.⁴² In the simplest form of the method, the 8×8 retarded surface Green's function $G(\mathbf{k}, \omega)$ is obtained by self-consistent calculation of $G(\mathbf{k}, \omega)$ and a transfer matrix $T(\mathbf{k}, \omega)$ as^{26,42}

$$G^{-1} = g^{-1} - H_z^\dagger T, \quad (13a)$$

$$T = G H_z, \quad (13b)$$

where $g = [zI_{8 \times 8} - H_{\text{SC}}(\mathbf{k})]^{-1}$ ($z = \omega + i\eta$) is the retarded Green's function for an isolated layer. η is the positive infinitesimal 0^+ , which is replaced by a small positive number in realistic calculations. Self-consistent calculation of the Green's function starts with $G = g$. The surface Green's

function could also be obtained in terms of other iteration schemes, such as the algorithm in Ref. 42. We have found no difference between the results obtained in terms of different iteration schemes.

After the retarded Green's functions are at hand, the spectral function is obtained as

$$A(\mathbf{k}, \omega) = -\sum_{i=1}^4 \text{Im} G_{ii}(\mathbf{k}, \omega) / \pi. \quad (14)$$

Since we have now two orbital and two spin degrees of freedom, there are many possible pairing channels for different possible pairing mechanisms. Realistic theoretical determination of the pairing symmetry requires the knowledge of pairing mechanism and reasonable parameter values, which are both lacking presently.²³ Here we will consider singlet and triplet pairing orders as phenomenological input parameters. Their qualitative differences in spectral functions could help to identify the pairing symmetry from experiments.

B. Gap opening in the topological surface states

Before presenting the full spectral function, we first would like to examine what happens to the topological surface states inherited from the normal state²⁰ upon the formation of a certain bulk pairing. The most salient feature of the topological insulator is the presence of gapless surface states (3D) or edge states (2D).^{1,2,7,39} In the case of $\text{Cu}_x\text{Bi}_2\text{Se}_3$, it is found that these surface states in the non-superconducting Bi_2Se_3 persist to the superconducting copper intercalated samples and are well separated from the bulk conduction band and hence well defined.^{19,20} It is thus an interesting question what would happen to them if a certain pairing forms in the bulk. In this subsection, we give a simple criterion to judge whether a gap would be induced in the topological surface states for an arbitrary bulk pairing.

Suppose the chemical potential lies slightly above the bottom of the bulk conduction band where the topological surface states are well separated and well defined.²⁰ If a pairing is realized in the topological surface states, it should occur between the two time-reversal related states for \mathbf{k} and $-\mathbf{k}$.¹⁷

We first consider model I. For our purpose, we will concentrate on the positive energy branch of the topological surface states. When the pairing occurs in the valence band,^{21,22} the analysis and conclusion would be similar. Since pairing occurs in the (k_x, k_y) space, we would ignore the z dependence of the surface modes when analyzing pairing properties. From the basis and the effective model obtained in Sec. II, the two eigenvectors for a certain 2D wave vector are

$$\eta_\alpha(\mathbf{k}) = \frac{1}{\sqrt{2}} \left[1, 0, \alpha \frac{k_+}{k}, 0 \right]^T, \quad (15)$$

where α is “+” (“−”) for the upper (lower) branch of the surface states, $k_\pm = k_x \pm i k_y$, $k = \sqrt{k_x^2 + k_y^2}$. The annihilation operators of these states are

$$d_{\mathbf{k}\alpha} = \frac{1}{\sqrt{2}} \left[c_{1\mathbf{k}\uparrow} + \frac{\alpha k_+}{k} c_{1\mathbf{k}\downarrow} \right]. \quad (16)$$

If pairing is induced in the upper surface conduction band at \mathbf{k} , the only possible pairing would be proportional to

$d_{\mathbf{k}+}^\dagger d_{-\mathbf{k}+}^\dagger$.¹⁷ Denote the time-reversal operator as \mathcal{T} .^{17,40} Since $\mathcal{T} c_{1\mathbf{k}\uparrow}^\dagger \mathcal{T}^{-1} = c_{1-\mathbf{k}\downarrow}^\dagger$ and $\mathcal{T} c_{1\mathbf{k}\downarrow}^\dagger \mathcal{T}^{-1} = -c_{1-\mathbf{k}\uparrow}^\dagger$, we have $\mathcal{T} d_{\mathbf{k}+}^\dagger d_{-\mathbf{k}+}^\dagger \mathcal{T}^{-1} = \frac{k_+}{k} d_{\mathbf{k}+}^\dagger d_{-\mathbf{k}+}^\dagger$. To ensure the time-reversal symmetry of the pairing, the actual pairing should be of the form

$$\begin{aligned} \hat{\Delta}_{\text{SCB}}^{\text{I}}(\mathbf{k}) &= \Delta_0 \frac{k_+}{k} d_{\mathbf{k}+}^\dagger d_{-\mathbf{k}+}^\dagger \\ &= \frac{\Delta_0}{2} \left[\frac{k_+}{k} c_{1\mathbf{k}\uparrow}^\dagger c_{1-\mathbf{k}\uparrow}^\dagger - \frac{k_-}{k} c_{1\mathbf{k}\downarrow}^\dagger c_{1-\mathbf{k}\downarrow}^\dagger \right. \\ &\quad \left. + (c_{1\mathbf{k}\downarrow}^\dagger c_{1-\mathbf{k}\uparrow}^\dagger - c_{1\mathbf{k}\uparrow}^\dagger c_{1-\mathbf{k}\downarrow}^\dagger) \right], \end{aligned} \quad (17)$$

where Δ_0 is the real pairing amplitude, which could be an even or odd real function of \mathbf{k} depending on the pairing realized in the bulk. “SCB” is an abbreviation for the surface conduction band (the topological surface states). Thus, the surface conduction band only supports the antiphase $p_x \pm i p_y$ equal-spin triplet pairing and the spin-singlet pairing within orbital 1. No other bulk pairing channels, especially those interorbital pairings, would open a gap in the topological surface states within the framework of model I.

For model II, the two eigenvectors of the surface states for a certain 2D wave vector are (again, ignoring the z dependence)

$$\eta_\alpha(\mathbf{k}) = \frac{1}{2} \left[1, -i, \alpha \frac{k_+}{k}, i \alpha \frac{k_-}{k} \right]^T, \quad (18)$$

where α is “+” (“−”) for the upper (lower) branch of the topological surface states. Following the same arguments as for the first model, when the chemical potential cuts the upper branch of these well-defined surface states the time-reversal invariant pairing is of the form

$$\begin{aligned} \hat{\Delta}_{\text{SCB}}^{\text{II}}(\mathbf{k}) &= \Delta_0 \frac{k_+}{k} d_{\mathbf{k}+}^\dagger d_{-\mathbf{k}+}^\dagger = \frac{\Delta_0}{4} \left[\frac{k_+}{k} (c_{1\mathbf{k}\uparrow}^\dagger c_{1-\mathbf{k}\uparrow}^\dagger - c_{2\mathbf{k}\uparrow}^\dagger c_{2-\mathbf{k}\uparrow}^\dagger) \right. \\ &\quad - \frac{k_-}{k} (c_{1\mathbf{k}\downarrow}^\dagger c_{1-\mathbf{k}\downarrow}^\dagger - c_{2\mathbf{k}\downarrow}^\dagger c_{2-\mathbf{k}\downarrow}^\dagger) \\ &\quad + i \frac{k_+}{k} (c_{1\mathbf{k}\uparrow}^\dagger c_{2-\mathbf{k}\uparrow}^\dagger + c_{2\mathbf{k}\uparrow}^\dagger c_{1-\mathbf{k}\uparrow}^\dagger) \\ &\quad + i \frac{k_-}{k} (c_{1\mathbf{k}\downarrow}^\dagger c_{2-\mathbf{k}\downarrow}^\dagger + c_{2\mathbf{k}\downarrow}^\dagger c_{1-\mathbf{k}\downarrow}^\dagger) \\ &\quad + (c_{1\mathbf{k}\downarrow}^\dagger c_{1-\mathbf{k}\uparrow}^\dagger - c_{1\mathbf{k}\uparrow}^\dagger c_{1-\mathbf{k}\downarrow}^\dagger + c_{2\mathbf{k}\downarrow}^\dagger c_{2-\mathbf{k}\uparrow}^\dagger - c_{2\mathbf{k}\uparrow}^\dagger c_{2-\mathbf{k}\downarrow}^\dagger) \\ &\quad \left. + i (c_{1\mathbf{k}\uparrow}^\dagger c_{2-\mathbf{k}\downarrow}^\dagger + c_{1\mathbf{k}\downarrow}^\dagger c_{2-\mathbf{k}\uparrow}^\dagger - c_{2\mathbf{k}\uparrow}^\dagger c_{1-\mathbf{k}\downarrow}^\dagger - c_{2\mathbf{k}\downarrow}^\dagger c_{1-\mathbf{k}\uparrow}^\dagger) \right]. \end{aligned} \quad (19)$$

As in Eq. (17), Δ_0 could be a constant or a real function of \mathbf{k} compatible with the symmetry of one pairing component contained in the above decomposition. Besides the intraorbital pairing channels active in model I, there are two additional interorbital pairing channels that are effective in producing a gap in the topological surface states. The last term in the above equation is just the odd-parity interorbital triplet pairing proposed by Fu and Berg²³ as a possible candidate of a topological superconductor to be realized in a superconductor such as $\text{Cu}_x\text{Bi}_2\text{Se}_3$.

The clear difference between $\hat{\Delta}_{\text{SCB}}^{\text{I}}$ and $\hat{\Delta}_{\text{SCB}}^{\text{II}}$ makes the distinction between model I and model II more obvious. Since the gap opening of the surface states is measurable, it is highly desirable to ascertain which model is the correct description of the underlying physics of Bi_2Se_3 and Bi_2Te_3 .

Previously, a simple effective model calculation indicated that no gap opens in the topological surface states for any triplet pairing induced by the proximity effect on the surface of a topological insulator.⁴¹ However, our analysis above indicates that if the proximity-induced triplet pairing is compatible with any of the triplet components explicit in $\hat{\Delta}_{\text{SCB}}^{\text{I}}$ ($\hat{\Delta}_{\text{SCB}}^{\text{II}}$) for model I (model II), then a full pairing gap could still be opened in the topological surface states. Note that the real gap opening pattern in the topological surface states also depends on Δ_0 .

Except for the pairing channels explicit in $\hat{\Delta}_{\text{SCB}}^{\text{I}}$ for model I and $\hat{\Delta}_{\text{SCB}}^{\text{II}}$ for model II, no other bulk pairing could open a gap in the topological surface states. The existence of surface Andreev bound states depends on whether or not a gap opens in the topological surface states. We clarify this matter in the next section.

C. Spectral function for typical pairing symmetries

Observation of superconductivity in $\text{Cu}_x\text{Bi}_2\text{Se}_3$ brings about anticipation that nontrivial topological superconducting states might be realized in this material. The topological superconductor is defined as a state with a full pairing gap in the bulk and nontrivial gapless Andreev bound states on the surface.²³

Possible pairings realizable in a system depend on the symmetry of the system and the specific pairing mechanism. In the case of pairing induced by short-range electron density-density interactions, Fu and Berg identified four possible pairing channels.²³ However, if the pairing is induced by more long-range interactions, such as the electron-phonon interaction, other pairing channels (e.g., in which the pairing potential is \mathbf{k} dependent) would also be possible. In the following we will analyze several typical pairings and compare results of the two different models. In each case, there are three typical situations as regards the position of the chemical potential μ : (1) μ lies in the bulk gap; (2) μ lies above but close to the bottom of the bulk conduction band, where the topological surface states are well separated from the continuum bulk conduction band; (3) μ lies far above the bulk conduction band bottom, where the surface states have merged into the continuum conduction band. While the latter two cases are relevant to the superconducting state of $\text{Cu}_x\text{Bi}_2\text{Se}_3$,^{19,20} the first case could be regarded as mimicking the proximity effect from an external superconductor.^{17,18,41} In this paper we would focus on the latter two situations. When the chemical potential lies in the valence band,^{21,22} the results should be qualitatively similar for the same type of bulk pairing.

Follow Wang *et al.*,²⁶ the model parameters are taken as $t = t_z = 0.5$, $m = -0.7$ in most cases. 0.7 is half of the bulk band gap. The width of the bulk conduction band at $k_x = k_y = 0$ is $2(2t_z - |m|) = 0.6$. The small positive number η in the Green's functions is taken as 10^{-4} .

Even-parity intraorbital singlet pairing. First, we study the simplest possible pairing denoted by $\underline{\Delta}(\mathbf{k}) = i\Delta_0 s_2 \otimes \sigma_0$. Spectral functions for the two different models are the same

for this pairing, so only one is presented in Fig. 1. Here and in the following, the degree of darkness indicates the intensity of the spectrum. The continuum portions of spectrum are contributions from the bulk states, which have small finite amplitudes on the surface. Henceforth, they will be called the bulk conduction band for simplicity. The contributions from the topological surface states are somewhat speckled because we have taken a finite grid in the (\mathbf{k}, ω) plane to calculate the spectral function. When the grid points are taken to be very dense, contributions from the topological surface states will also become smooth. To see the qualitative behavior more clearly, a reasonably large pairing amplitude $\Delta_0 = 0.1$ is considered.²⁰ The result is nearly identical in the ΓK direction (along k_x axis) and the ΓM direction (along k_y axis) of the 2D reduced Brillouin zone (BZ). The topological surface states of both models open a gap, which is consistent with the

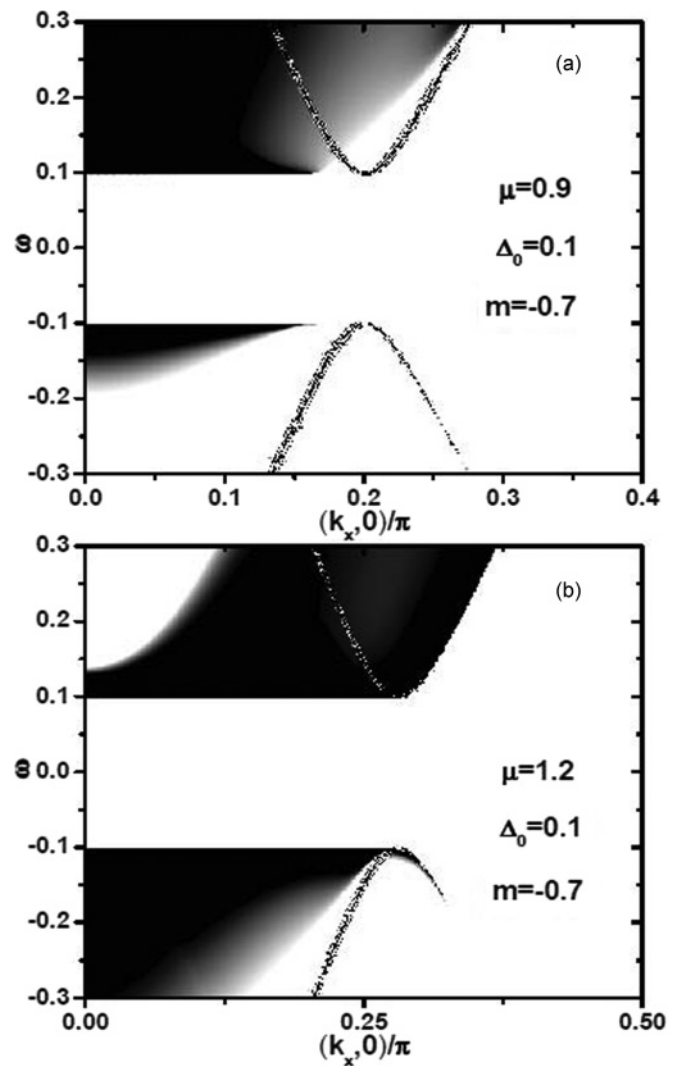


FIG. 1. Spectral function for even-parity intraorbital s -wave pairing, for two typical parameter sets for which the topological surface states at the chemical potential (a) are well separated from the bulk conduction band and (b) merge into the bulk conduction band. The two models give identical results for this pairing. Spectra along other directions (crossing the Γ point) are qualitatively identical.

analysis of the previous subsection. Since no Andreev bound state exists, this pairing is topologically trivial. The other intraorbital singlet pairings with a \mathbf{k} -dependent Δ_0 , which is an even function of \mathbf{k} , can also be considered, such as the $d_{x^2-y^2}$ -wave pairing. In these cases, there will be line nodes along the nodal directions of the pairing gap.

Even-parity interorbital singlet pairing. Since there are now two orbits, another singlet pairing exists in the interorbital channel. The pairing matrix for the s -wave case is $\underline{\Delta}(\mathbf{k}) = i\Delta_0 s_2 \otimes \sigma_1$. The corresponding spectral functions presented in Fig. 2 for this pairing are still identical for the two models. They differ from the spectra of the former intraorbital pairing channel in at least two aspects. First, no gap opens in the topological surface states, which is in agreement with the criterion proposed in the previous subsection. Second, although a full gap also opens in the continuum part of the spectrum, it is not constant and shows some \mathbf{k} dependence. As shown in Fig. 2(b), the continuum part of the spectrum even nearly closes at some special wave vectors for certain parameters. Another interesting feature is the strong redistribution of spectral weight between the continuum conduction band and the topological surface states. Some weight in the bulk conduction band part of the surface spectrum above the chemical potential is depleted and transferred to the topological surface states below the chemical potential. This redistribution arises from the particle-hole mixing induced by the presence of bulk superconducting pairing. As we will see below, a similar feature is present for each bulk pairing that does not open a gap in the topological surface states.

Odd-parity interorbital triplet pairing. We now consider the odd-parity interorbital triplet pairing channel proposed by Fu and Berg as a candidate for possible nontrivial topological superconducting states in $\text{Cu}_x\text{Bi}_2\text{Se}_3$.²³ The pairing matrix is $\underline{\Delta}(\mathbf{k}) = \Delta_0 s_1 \otimes \sigma_2$. As is shown in Fig. 3, the spectral functions for the two models differ greatly. When the chemical potential is close to bottom of the bulk conduction band, the surface conduction band is still gapless for model I but opens a gap for model II, in agreement with the analysis in the above subsection. Another essential difference is the existence or nonexistence of Andreev bound states. For model I, a band of Andreev bound states appears inside of the insulating gap of the continuum which continuously connects to the topological surface states, while for model II, there is a point node at $(0, 0)$ and no Andreev bound state exists inside of the gap region. When the chemical potential is increased to the position where the surface conduction band has almost merged into the continuum part of the surface spectrum (corresponding to a contribution from the bulk conduction band), the surface spectra for the two models are as shown in Fig. 4. Since now there is no well-separated surface conduction band, a full gap opens also for model I. However, a band of Andreev bound states still exists. When we further increase the chemical potential to $\mu > 1.3$ (for $m = -0.7$), there is no state close to the Γ point, and thus there will be no Andreev bound state even for model I. A strong redistribution of spectral weight arising from the particle-hole mixing between the continuum bulk conduction band and the topological surface states is observed in the results for model I.

Besides the pairing studied above, there are also other odd-parity pairings. Since they are possibly related to nontrivial

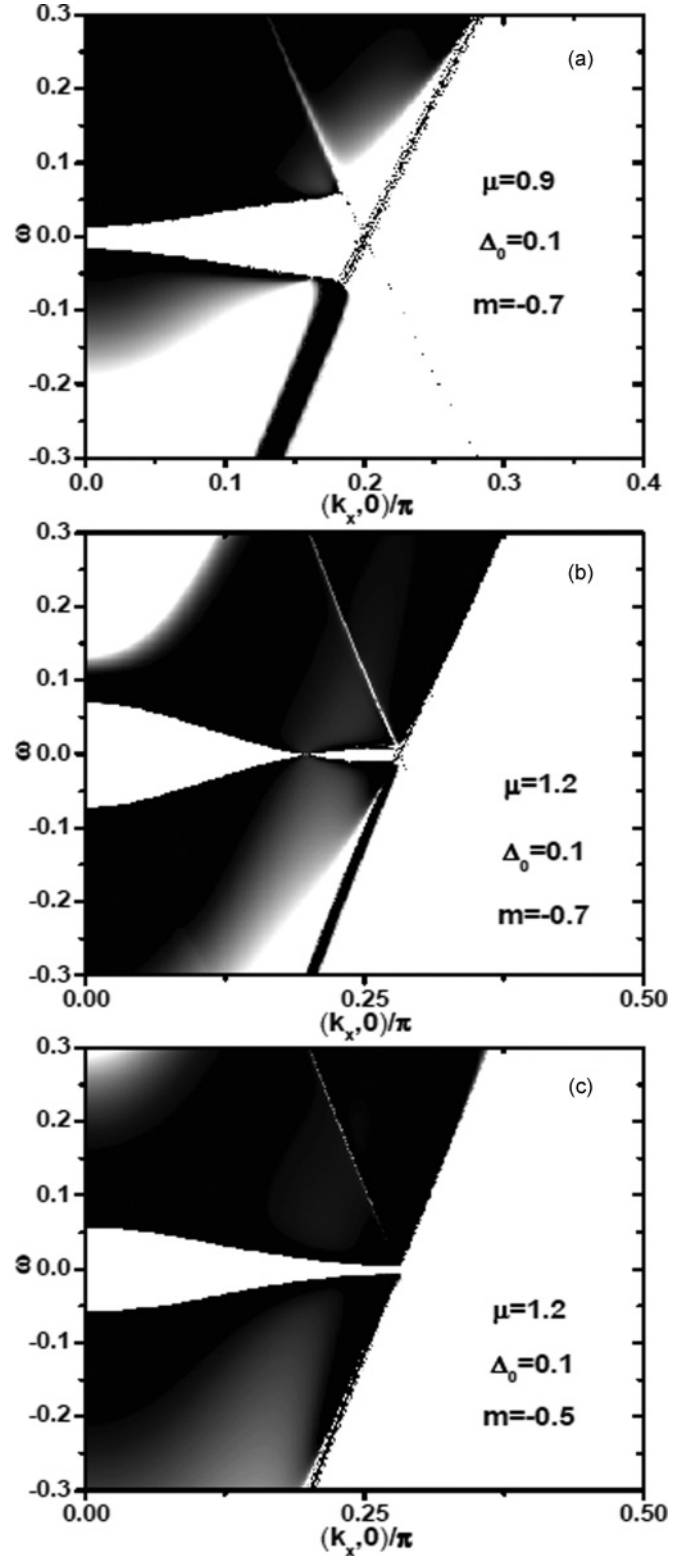


FIG. 2. Spectral function for even-parity interorbital s -wave pairing, for three sets of parameters for which at the chemical potential (a) the topological surface states are well separated from the bulk conduction band, (b) the topological surface states are almost merged into the bulk conduction band, and (c) the topological surface states are well merged into the bulk conduction band. The two models give identical results for this pairing. Spectra along other directions (crossing the Γ point) are qualitatively identical.

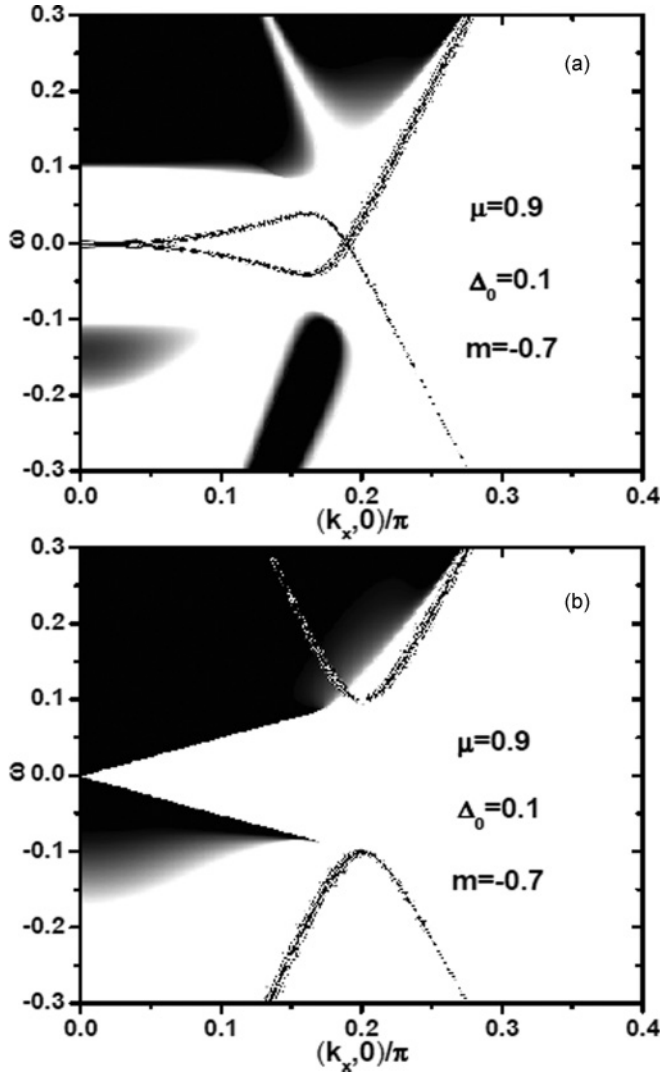


FIG. 3. Spectral function for odd-parity interorbital triplet pairing in the opposite spin pairing channel, for (a) model I and (b) model II. Shown are the cases for which the topological surface states are well separated from the bulk conduction band at the chemical potential. The parameters are as shown on the figures. Spectra along other directions (crossing the Γ point) are qualitatively identical.

topological superconducting phases, we analyze several of them in the following.

Odd-parity intraorbital singlet pairing. In this case, every orbital pairs into a spin singlet, but the two orbitals have a relative π phase difference and are hence odd in parity.²³ The pairing matrix is denoted as $\underline{\Delta}(\mathbf{k}) = i\Delta_0 s_2 \otimes \sigma_3$. The corresponding spectral functions for the two models are presented in Figs. 5(a) and 5(b) for chemical potential close to the bottom of the bulk conduction band and thus the topological surface state is well defined. A comparison with the previous pairing, shown in Figs. 3 and 4, indicates that the results are interchanged between the two models. Gap opening in the topological surface states again follows the expectation from the previous subsection. The Andreev bound states in the bulk band gap for the second model again connect continuously to the protected topological surface states. The behaviors for higher chemical potentials, as shown in Figs. 5(c) and 5(d),

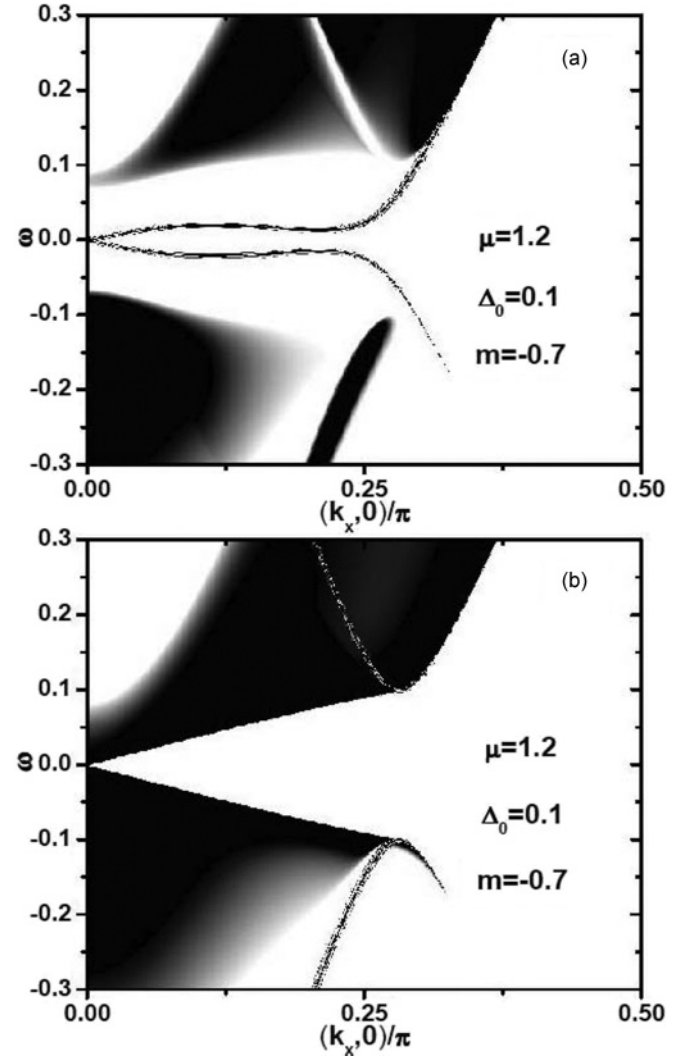


FIG. 4. Spectral function for odd-parity interorbital triplet pairing in the opposite spin pairing channel, for (a) model I and (b) model II. Shown are the cases for which the topological surface states are merged into the bulk conduction band at the chemical potential. The parameters are as shown on the figures. Spectra along other directions (crossing the Γ point) are qualitatively identical.

are similar to that of the previous pairing shown in Fig. 4 with the two models interchanged.

Odd-parity interorbital equal-spin triplet pairing. Another interesting possibility is the equal-spin pairing channel. Here we consider the twofold degenerate interorbital pairing channels as proposed by Fu and Berg.²³ This kind of pairing could be favored by interorbital ferromagnetic Heisenberg interactions.⁴³ The two independent choices for the pairing matrix are $\underline{\Delta}^{(1)}(\mathbf{k}) = i\Delta_0 s_0 \otimes \sigma_2$ and $\underline{\Delta}^{(2)}(\mathbf{k}) = \Delta_0 s_3 \otimes \sigma_2$. For these pairings, it is easy to see that no gap opens in the topological surface states for both models. Since results for the two models are identical, we only show those for model I. As shown in Fig. 6 for $\underline{\Delta}^{(1)}(\mathbf{k})$, a peculiar anisotropic Andreev bound state structure is observed. An important difference of this pairing from the above odd-parity pairing channels is that it is anisotropic with respect to k_x and k_y . Although the bulk dispersion is gapless in the $k_y k_z$ [$k_x k_z$] plane for $\underline{\Delta}^{(1)}(\mathbf{k})$ [$\underline{\Delta}^{(2)}(\mathbf{k})$],

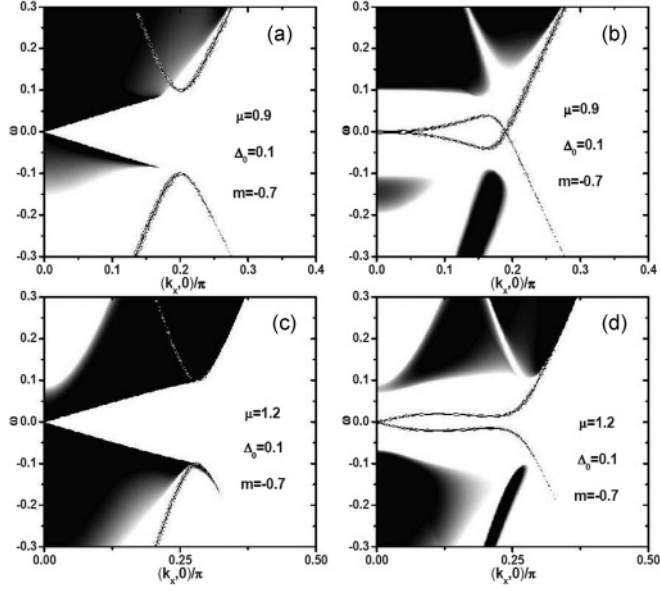


FIG. 5. Spectral function for odd-parity intraorbital s -wave pairing, for model I [(a) and (c)] and model II [(b) and (d)]. For (a) and (b) [(c) and (d)], the topological surface states are well separated from [merged into] the bulk conduction band at the chemical potential. Spectra along other directions (crossing the Γ point) are qualitatively identical.

there is still a band of Andreev bound states for the wave vectors smaller than k_F where a gap opens. The peculiar feature of the Andreev bound states along k_y [k_x] for $\Delta^{(1)}(\mathbf{k})$ [$\Delta^{(2)}(\mathbf{k})$] is that they are dispersionless (that is, completely flat).

Besides the Andreev bound states within the gap, the redistribution of spectral weights arising from the particle-hole mixing is also very interesting. An important feature is the appearance of a linear band beyond the Fermi momentum

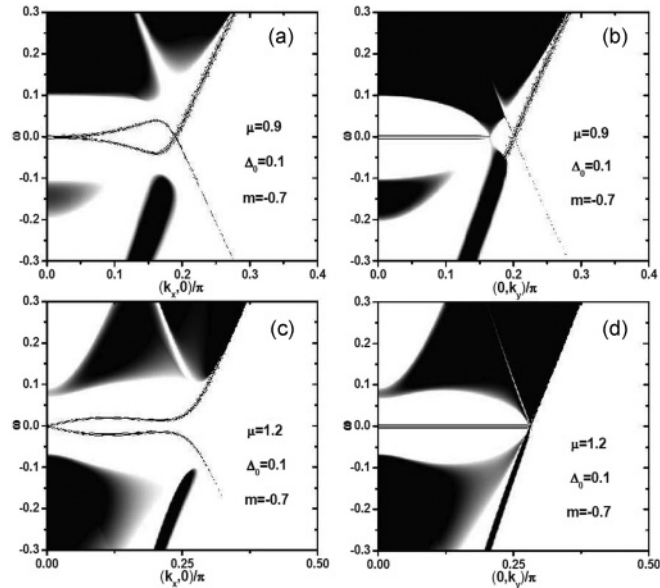


FIG. 6. Spectral function for odd-parity interorbital triplet pairing in the equal spin pairing channel, for model I and $\Delta^{(1)}(\mathbf{k}) = i\Delta_0 s_0 \otimes \sigma_2$. (a) and (c) are along the k_x direction while (b) and (d) are along the k_y direction. The parameters are as shown on the figure.

TABLE I. Summary of results for the bulk pairings considered explicitly in the present work. Results for two models, I and II, are compared. “TSS” and “ABS” are the abbreviations for “topological surface states” and “Andreev bound states,” respectively. “+” and “−” mean the even-parity and odd-parity pairings. For “Gap in TSS,” “Y” and “N” represent that a gap could and could not open in the topological surface states. For “ABS,” “Y” and “N” denote that Andreev bound states exist and do not exist on the surface for a certain bulk pairing.

$\Delta(\mathbf{k})$	$is_2 \otimes \sigma_0$	$is_2 \otimes \sigma_1$	$s_1 \otimes \sigma_2$	$is_2 \otimes \sigma_3$	$is_0 \otimes \sigma_2$
P	+	+	−	−	−
Gap in TSS: I	Y	N	N	Y	N
Gap in TSS: II	Y	N	Y	N	N
ABS: I	N	N	Y	N	Y
ABS: II	N	N	N	Y	Y

and below the chemical potential, existing as a particle-hole symmetric band of the original topological surface states in the normal phase. Once a bulk superconducting pairing forms in the topological insulator itself (and not in the intercalated copper) in $\text{Cu}_x\text{Bi}_2\text{Se}_3$, such a linear dispersive band is always there, no matter whether a gap opens or not in the topological surface states. To see the above feature more clearly, we show in Figs. 7(a) and 7(b) the energy distribution curves (EDC) for several typical wave vectors for two typical pairings and parameter sets, which are the same as those of Figs. 1(a) and 3(a), respectively. The linear band mentioned above appears as a well-defined peak slightly below the chemical potential. As the wave vector increases and shifts away from the Fermi momentum, the peak deviates linearly from the chemical potential and the height and width of it both decrease rapidly, which is in agreement with the fact that superconducting pairing forms only close to the chemical potential. The integrated weight of the linearly dispersive peaks in Figs. 7(a) and 7(b) are shown in Fig. 7(c), as a function of the wave vector. If the gap in the superconductors realized from a topological insulator is larger than what is reported in Ref. 20, the above linear dispersive structure in the EDC could be detectable by ARPES for the wave vectors close enough to the Fermi momentum.^{19,20} Then this well-defined peak structure arising from the topological surface states could be used as a good indicator of the formation of superconducting correlation in Bi_2Se_3 and the involvement of the topological surface states in the superconducting phase.

From the above results for five different pairing symmetries, we observe a simple rule for the existence of nontrivial surface Andreev bound states. For odd-parity pairings, when a full gap opens in the continuum part of the surface spectrum but no gap opens in the topological surface states, a band of surface Andreev bound states would arise which traverses the bulk pairing gap. This criterion is verified also by calculations for other superconducting pairings not presented here. The results in this subsection are summarized in Table I.

D. The surface Andreev bound states

For some superconducting pairings, such as the $p \pm ip$ wave pairing, it was known that Majorana fermions exist as

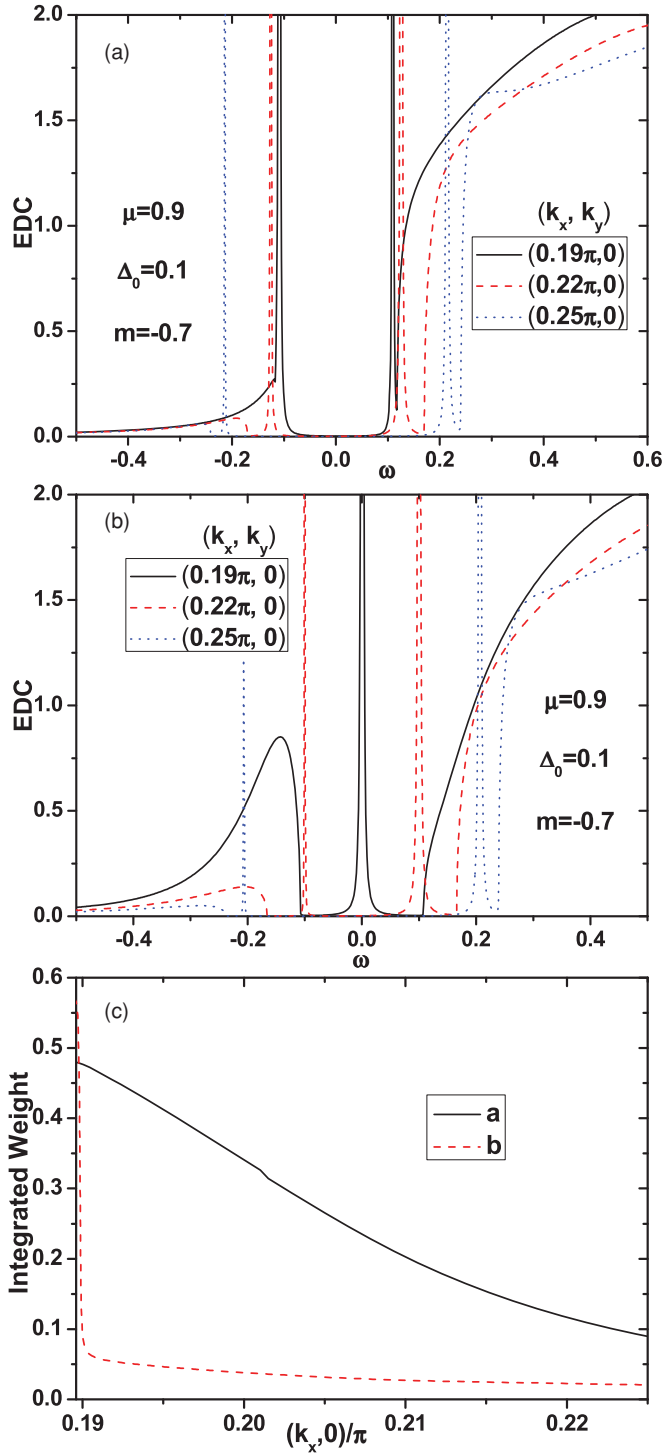


FIG. 7. (Color online) EDC for three typical wave vectors for (a) even-parity intraorbital singlet pairing [with parameters the same as in Fig. 1(a)] and (b) odd-parity interorbital triplet pairing [with parameters the same as in Fig. 3(a)] within model I. The parameters are as shown on the figures. (c) The integrated weight of the linearly dispersive peaks slightly below the chemical potential with parameters corresponding to (a) and (b), respectively.

gapless surface or edge modes.⁴⁰ According to an argument by Linder *et al.*, all zero-energy Andreev bound states emerging from the nondegenerate (that is, on each surface) topological surface states should be Majorana fermions.⁴¹ As regards our

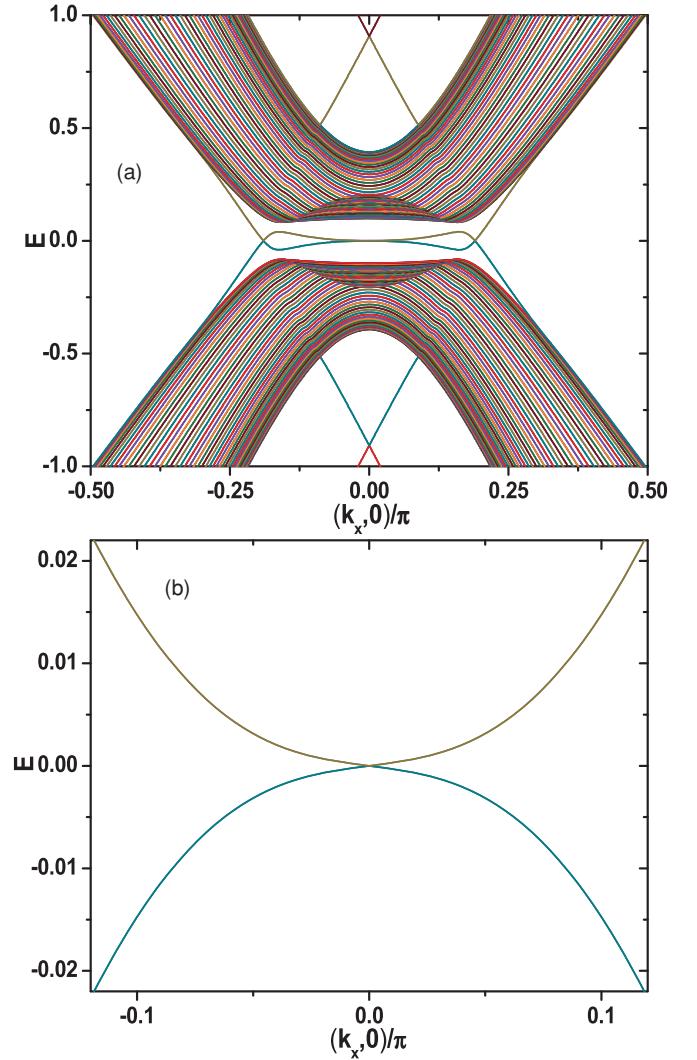


FIG. 8. (Color online) (a) Dispersion of a 50-layer superconductor emerging from model I and for the odd-parity interorbital triplet pairing $\underline{\Delta}(\mathbf{k}) = \Delta_0 s_1 \otimes \sigma_2$. Parameters used are $\mu = 0.9$, $\Delta_0 = 0.1$, and $m = -0.7$. (b) An enlargement of the small-wave-vector and low-energy part of (a).

case, in the parameter region where the topological surface states are well separated from the bulk conduction band, one observation is that the surface Andreev bound states in the gap region connect continuously to the topological surface states inherited from the normal phase [e.g., Fig. 3(a)]. Since the topological surface states are spin-polarized helical and nondegenerate, the surface Andreev bound states on each surface should also be nondegenerate. Then according to the arguments by Linder *et al.*,⁴¹ the zero-energy Andreev bound states presented in the above section should also be Majorana fermions.

To see more clearly the properties of the surface Andreev bound states, we perform numerical calculations on a finite-layer superconducting film. As an example, we will analyze the odd-parity interorbital triplet pairing channel described by $\underline{\Delta}(\mathbf{k}) = \Delta_0 s_1 \otimes \sigma_2$, within model I. Figure 8(a) shows the dispersion for a 50-layer film. It reproduces all the basic features in the spectral function [see Fig. 3(a)]. Enlargement

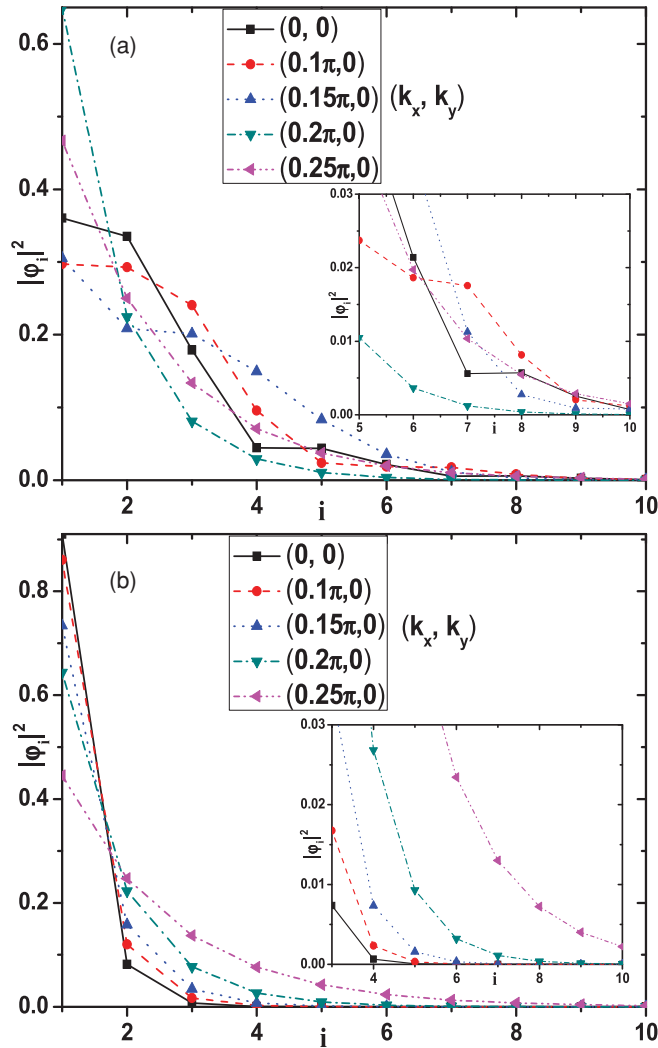


FIG. 9. (Color online) (a) Decay of the wave function amplitude with layer number for the surface Andreev bound states localized on the top several layers; results are obtained for the superconducting state emerging from model I and for the odd-parity interorbital triplet pairing $\underline{\Delta}(\mathbf{k}) = \Delta_0 s_1 \otimes \sigma_2$. The parameters are $\mu = 0.9$, $\Delta_0 = 0.1$, and $m = -0.7$. The Fermi wave vector in the k_x direction is about 0.19π . (b) Decay of the wave function amplitude with layer number for the topological surface states localized on the top several layers, for the normal states of model I with $m = -0.7$. The two insets show enlargements of the small-amplitude regions of the two figures.

of the low-energy dispersion [Fig. 8(b)] shows that dispersion of the surface Andreev bound states is linear close to the Γ point. For all the bulk pairings studied above, the dispersion for the superconducting film reproduces well the features of the corresponding spectral function. Figure 9(a) shows the wave function amplitudes for the surface state localized on the top several layers. The corresponding behavior for the topological surface states in the normal phase is presented

in Fig. 9(b). The decay behavior of the surface bound states into the bulk in Fig. 9(a) is seen to change continuously from oscillatory exponential decay in the gap region²³ to monotonic exponential decay outside the gap region. That is, the state changes from particle-hole mixed superconducting quasiparticle to the topological surface states in the normal phase.

In this paper, we have been discussing a homogeneous phase both in the bulk and on the surface. However, in the presence of exotic surface excitations such as vortices, novel Majorana fermion modes may appear in the vortex core even for bulk pairings with no surface Andreev bound states. There have already been many papers focusing on this possibility, which usually start from the effective model.^{43–45}

The Andreev bound states that appear in many different superconducting pairings as shown above confirm the idea that superconducting states realized in a topological insulator very probably have nontrivial topological characters. The Andreev bound states, if they exist, should be easily detectable in tunneling-type experiments as a well-defined zero-energy peak. Another way to detect the Majorana fermions as zero-energy Andreev bound states is to take advantage of the various phase-sensitive transport devices proposed to produce and manipulate the Majorana fermions.^{17,46}

IV. SUMMARY

In this paper, we have discussed the surface spectral function of superconductors realized from a topological insulator, such as copper-intercalated Bi_2Se_3 . These functions are calculated by projecting bulk states to the surface for two different models used previously for the topological insulator. Dependence of the surface spectra on the symmetry of the bulk pairing order parameter is discussed with particular emphasis on the odd-parity pairing. When an odd-parity pairing opens a full gap in the bulk, but not for the topological surface states, zero-energy Andreev bound states are shown to appear on the surface. When the topological surface states are well separated from the bulk conduction band, the redistribution of spectral weight induced by the onset of superconductivity produces a linearly dispersive peak structure beyond the Fermi momentum and below the chemical potential. This is proposed as a criterion for confirming that superconductivity occurs in Bi_2Se_3 (and not in copper) and that the topological surface states are involved in the superconducting phase. The zero-energy surface Andreev bound states are argued to be Majorana fermions.

ACKNOWLEDGMENTS

We thank Peter Thalmeier for helpful discussions. This work was supported by NSC Grant No. 98-2112-M-001-017-MY3. Some of the calculations were performed at the National Center for High-Performance Computing in Taiwan.

¹C. L. Kane and E. J. Mele, *Phys. Rev. Lett.* **95**, 146802 (2005); **95**, 226801 (2005).

²B. Andrei Bernevig, Taylor Hughes, and Shou-Cheng Zhang, *Science* **314**, 1757 (2006).

³D. N. Sheng, Z. Y. Weng, L. Sheng, and F. D. M. Haldane, *Phys. Rev. Lett.* **97**, 036808 (2006).

⁴Markus König, Steffen Wiedmann, Christoph Brüne, Andreas Roth, Hartmut Buhmann, Laurens W. Molenkamp,

- Xiao-Liang Qi, and Shou-Cheng Zhang, *Science* **318**, 766 (2007).
- ⁵J. E. Moore and L. Balents, *Phys. Rev. B* **75**, 121306 (2007).
- ⁶R. Roy, *Phys. Rev. B* **79**, 195322 (2009).
- ⁷Liang Fu, C. L. Kane, and E. J. Mele, *Phys. Rev. Lett.* **98**, 106803 (2007).
- ⁸Liang Fu and C. L. Kane, *Phys. Rev. B* **76**, 045302 (2007).
- ⁹D. Hsieh, D. Qian, L. Wray, Y. Xia, Y. S. Hor, R. J. Cava, and M. Z. Hasan, *Nature (London)* **452**, 970 (2008).
- ¹⁰Xiao-Liang Qi, Taylor L. Hughes, and Shou-Cheng Zhang, *Phys. Rev. B* **78**, 195424 (2008).
- ¹¹Y. Xia, D. Qian, D. Hsieh, L. Wray, A. Pal, H. Lin, A. Bansil, D. Grauer, Y. S. Hor, R. J. Cava, and M. Z. Hasan, *Nature Phys.* **5**, 398 (2009).
- ¹²Haijun Zhang, Chao-Xing Liu, Xiao-Liang Qi, Xi Dai, Zhong Fang, and Shou-Cheng Zhang, *Nature Phys.* **5**, 438 (2009).
- ¹³M. Z. Hasan and C. L. Kane, *Rev. Mod. Phys.* **82**, 3045 (2010).
- ¹⁴Xiao-Liang Qi and Shou-Cheng Zhang, e-print [arXiv:1008.2026](#) (to be published).
- ¹⁵Andreas P. Schnyder, Shinsei Ryu, Akira Furusaki, and Andreas W. Ludwig, *Phys. Rev. B* **78**, 195125 (2008).
- ¹⁶Frank Wilczek, *Nature Phys.* **5**, 614 (2009).
- ¹⁷Liang Fu and C. L. Kane, *Phys. Rev. Lett.* **100**, 096407 (2008); **102**, 216403 (2009).
- ¹⁸Jay D. Sau, Roman M. Lutchyn, Sumanta Tewari, and S. Das Sarma, *Phys. Rev. B* **82**, 094522 (2010).
- ¹⁹Y. S. Hor, A. J. Williams, J. G. Checkelsky, P. Roushan, J. Seo, Q. Xu, H. W. Zandbergen, A. Yazdani, N. P. Ong, and R. J. Cava, *Phys. Rev. Lett.* **104**, 057001 (2010).
- ²⁰L. Andrew Wray, Su-Yang Xu, Yuqi Xia, Yew San Hor, Dong Qian, Alexei V. Fedorov, Hsin Lin, Arun Bansil, Robert J. Cava, and M. Zahid Hasan, *Nature Phys.* **6**, 855 (2010).
- ²¹J. L. Zhang, S. J. Zhang, H. M. Weng, W. Zhang, L. X. Yang, Q. Q. Liu, S. M. Feng, X. C. Wang, R. C. Yu, L. Z. Cao, L. Wang, W. G. Yang, H. Z. Liu, W. Y. Zhao, S. C. Zhang, X. Dai, Z. Fang, and C. Q. Jin, e-print [arXiv:1009.3691v1](#).
- ²²Chao Zhang, Liling Sun, Zhaoyu Chen, Xingjiang Zhou, Qi Wu, Wei Yi, Jing Guo, Xiaoli Dong, and Zhongxian Zhao, e-print [arXiv:1009.3746](#) (to be published).
- ²³Liang Fu and Erez Berg, *Phys. Rev. Lett.* **105**, 097001 (2010).
- ²⁴Masatoshi Sato, *Phys. Rev. B* **81**, 220504(R) (2010); **79**, 214526 (2009).
- ²⁵Zhanybek Alpichshev, J. G. Analytis, J.-H. Chu, I. R. Fisher, Y. L. Chen, Z. X. Shen, A. Fang, and A. Kapitulnik, *Phys. Rev. Lett.* **104**, 016401 (2010).
- ²⁶Qiang-Hua Wang, Da Wang, and Fu-Chun Zhang, *Phys. Rev. B* **81**, 035104 (2010).
- ²⁷D. Hsieh, Y. Xia, D. Qian, L. Wray, J. H. Dil, F. Meier, J. Osterwalder, L. Patthey, J. G. Checkelsky, N. P. Ong, A. V. Fedorov, H. Lin, A. Bansil, D. Grauer, Y. S. Hor, R. J. Cava, and M. Z. Hasan, *Nature* **460**, 1101 (2009).
- ²⁸Binghai Yan, Chao-Xing Liu, Hai-Jun Zhang, Chi-Yung Yam, Xiao-Liang Qi, Thomas Frauenheim, and Shou-Cheng Zhang, *Europhys. Lett.* **90**, 37002 (2010).
- ²⁹K. Kuroda, M. Ye, A. Kimura, S. V. Ereemeev, E. E. Krasovskii, E. V. Chulkov, Y. Ueda, K. Miyamoto, T. Okuda, K. Shimada, H. Namatame, and M. Taniguchi, *Phys. Rev. Lett.* **105**, 146801 (2010).
- ³⁰Zhi Ren, A. A. Taskin, Satoshi Sasaki, Kouji Segawa, and Yoichi Ando, *Phys. Rev. B* **82**, 241306 (2010).
- ³¹Su-Yang Xu, L. A. Wray, Y. Xia, R. Shankar, A. Petersen, A. Fedorov, H. Lin, A. Bansil, Y. S. Hor, D. Grauer, R. J. Cava, and M. Z. Hasan, e-print [arXiv:1007.5111](#) (to be published).
- ³²Rundong Li, Jing Wang, Xiao-Liang Qi, and Shou-Cheng Zhang, *Nature Phys.* **6**, 284 (2010).
- ³³Chao-Xing Liu, Hai-Jun Zhang, Binghai Yan, Xiao-Liang Qi, Thomas Frauenheim, Xi Dai, Zhong Fang, and Shou-Cheng Zhang, *Phys. Rev. B* **81**, 041307(R) (2010).
- ³⁴Chao-Xing Liu, Xiao-Liang Qi, Haijun Zhang, Xi Dai, Zhong Fang, and Shou-Cheng Zhang, *Phys. Rev. B* **82**, 045122 (2010).
- ³⁵Hai-Zhou Lu, Wen-Yu Shan, Wang Yao, Qian Niu, and Shun-Qing Shen, *Phys. Rev. B* **81**, 115407 (2010).
- ³⁶Wen-Yu Shan, Hai-Zhou Lu, and Shun-Qing Shen, *New J. Phys.* **12**, 043048 (2010).
- ³⁷Liang Fu, *Phys. Rev. Lett.* **103**, 266801 (2009).
- ³⁸P. Larson, V. A. Greanya, W. C. Tonjes, Rong Liu, S. D. Mahanti, and C. G. Olson, *Phys. Rev. B* **65**, 085108 (2002).
- ³⁹Xiao-Liang Qi and Shou-Cheng Zhang, *Phys. Today* **63**(1), 33 (2010).
- ⁴⁰Xiao-Liang Qi, Taylor L. Hughes, and Shou-Cheng Zhang, *Phys. Rev. B* **81**, 134508 (2010).
- ⁴¹Jacob Linder, Yukio Tanaka, Takehito Yokoyama, Asle Sudbø, and Naoto Nagaosa, *Phys. Rev. Lett.* **104**, 067001 (2010).
- ⁴²M. P. López Sancho, J. M. López Sancho, and J. Rubio, *J. Phys. F* **14**, 1205 (1984); **15**, 851 (1985).
- ⁴³Luiz Santos, Titus Neupert, Claudio Chamon, and Christopher Mudry, *Phys. Rev. B* **81**, 184502 (2010).
- ⁴⁴Xiao-Liang Qi, Taylor L. Hughes, S. Raghu, and Shou-Cheng Zhang, *Phys. Rev. Lett.* **102**, 187001 (2009).
- ⁴⁵Pavan Hosur, Pouyan Ghaemi, Roger S. K. Mong, and Ashvin Vishwanath, e-print [arXiv:1012.0330](#) (to be published).
- ⁴⁶K. T. Law, Patrick A. Lee, and T. K. Ng, *Phys. Rev. Lett.* **103**, 237001 (2009).